

FINITE ELEMENT ANALYSIS OF REINFORCED CONCRETE SLABS UNDER SERVICE LOADING USING A NEW TRIANGULAR LAYERED PLATE ELEMENT

Yixia Zhang^{*}, Mark A. Bradford^{*} and R. Ian Gilbert^{*}

^{*} School of Civil and Environmental Engineering
The University of New South Wales
UNSW, Sydney, NSW 2052, Australia
e-mail: sarahyxzhang@unsw.edu.au, web page: <http://www.civeng.unsw.edu.au>

Key words: Concrete cracking, RC slabs, Tension stiffening, Triangular layered element.

Summary. *This paper develops a 3-node, 18-dof triangular layered plate element for the geometric and material nonlinear analysis of RC slabs at service loads. It combines a 9-dof triangular membrane element with drilling degrees of freedom and a refined, non-conforming 9-dof triangular plate bending element to account for membrane and flexural coupling. Two numerical examples illustrate the efficacy of this robust element.*

1 INTRODUCTION

In the FE analysis of RC engineering structures, recourse is usually made to either a modified stiffness approach or to a layered formulation. The latter is more popular, and forms the basis for the element derived herein. A large number of layered triangular and quadrilateral elements have been reported for the nonlinear analysis of plate/shell structures, including RC slabs, each with their own merits and drawbacks. However, it appears that an 18-dof triangular element for the nonlinear analysis of RC slabs has not been reported, and this paper presents the derivation of such an element that combines the 3-node, 9-dof membrane element of Allman¹ that includes drilling freedoms, and the RT9 non-conforming 3-node, 9-dof plate bending element of Cheung and Chen². The proposed element is simple in its formulation and it provides robust performance in numerical analysis. Its scope and accuracy is illustrated by modelling flat RC slabs tested elsewhere.

2 BASIC EQUATIONS

The RC slab is discretised into c concrete layers and s smeared steel layers, with perfect bond between each layer, so that variations of stresses throughout the depth $z \in [0, h]$ are approximated as being piecewise constant, with the Gauss points at the layer mid-thicknesses. Using Kirchhoff's thin-plate theory, the displacements of an arbitrary $P(x, y, z)$ within the element are

$$\Delta \hat{u} = \Delta u(x, y) - z \Delta w_{,x} ; \quad \Delta \hat{v} = \Delta v(x, y) - z \Delta w_{,y} ; \quad \Delta \hat{w} = \Delta w(x, y), \quad (1)$$

where Δu , Δv , Δw = translational displacement increments. The Green finite strain increments using von Karman's large deformation assumption are

$$\Delta \boldsymbol{\varepsilon} = \begin{Bmatrix} \Delta \varepsilon_x \\ \Delta \varepsilon_y \\ \Delta \varepsilon_{xy} \end{Bmatrix} = \begin{Bmatrix} \Delta \hat{u}_{,x} + \frac{1}{2}(\Delta \hat{u}_{,x}^2 + \Delta \hat{v}_{,x}^2 + \Delta \hat{w}_{,x}^2) \\ \Delta \hat{v}_{,y} + \frac{1}{2}(\Delta \hat{u}_{,y}^2 + \Delta \hat{v}_{,y}^2 + \Delta \hat{w}_{,y}^2) \\ \Delta \hat{u}_{,y} + \Delta \hat{v}_{,x} + \Delta \hat{u}_{,x} \Delta \hat{u}_{,y} + \Delta \hat{v}_{,x} \Delta \hat{v}_{,y} + \Delta \hat{w}_{,x} \Delta \hat{w}_{,y} \end{Bmatrix}, \quad (2)$$

which leads to

$$\Delta \boldsymbol{\varepsilon} = \Delta \hat{\boldsymbol{\varepsilon}} + z \Delta \hat{\boldsymbol{\chi}} = \Delta \mathbf{e} + \Delta \boldsymbol{\eta}, \quad (3)$$

where $\Delta \mathbf{e}$ = membrane strain increments, $\Delta \boldsymbol{\eta}$ = bending strain increments, and the second Piola-Kirchhoff stress increment $\Delta \boldsymbol{\sigma}$ can be found from the constitutive law $\mathbf{D}(\cdot)$ by

$$\Delta \boldsymbol{\sigma} = \mathbf{D}(\Delta \hat{\boldsymbol{\varepsilon}} + z \Delta \hat{\boldsymbol{\chi}}). \quad (4)$$

3 MATERIAL MODELLING

The onset of concrete cracking in tension is defined as being when the maximum principal stress (direction $\bar{\mathbf{1}}$) reaches the concrete tensile strength f_t which defines a crack perpendicular to $\bar{\mathbf{1}}$, and a second crack forms perpendicular to the minimum principal stress direction $\bar{\mathbf{2}}$ when this stress reaches f_t . At the first instant the material property matrix $\mathbf{D}'_c = \text{diag}[0, E_c, G_{c12}]$; in the second instant the property matrix becomes $\mathbf{D}'_c = \text{diag}[0, E_c, \frac{1}{2}G_{c12}]$, where E_c = Young's modulus and G_{c12} = shear modulus that accounts for aggregate interlock and dowel action. These take prescriptive formulations³, as does the effect of tension stiffening⁴.

4 UPDATED LAGRANGIAN FORMULATION

The linearised formulation of the principle of virtual work is represented by

$$\int_{V^{et}} \delta \Delta \mathbf{e}^T {}^t \mathbf{D} \Delta \mathbf{e} dV^{et} + \int_{V^{et}} \delta \Delta \boldsymbol{\eta}^T {}^t \boldsymbol{\sigma} dV^{et} = \delta \Delta \mathbf{W}^{t+\Delta t} - \int_{V^{et}} \delta \Delta \mathbf{e}^T {}^t \boldsymbol{\sigma} dV^{et}, \quad (5)$$

for times t and then Δt . The first term in (5) is $\delta \Delta \mathbf{q}'^e \mathbf{K}'^e \Delta \mathbf{q}'^e$, the second term is $\delta \Delta \mathbf{q}'^e \mathbf{K}_\sigma'^e \Delta \mathbf{q}'^e$, and the final term leads to the internal force vector $\delta \Delta \mathbf{q}'^e \mathbf{R}'^e$, where \mathbf{K}^e = element stiffness matrix, \mathbf{K}_σ^e = element geometric stiffness matrix and $\mathbf{W}^{t+\Delta t}$ = external force vector.

5 18-DOF 3-NODED TRIANGULAR ELEMENT

Using the representation of Allman¹, the displacement function at any point is

$$\begin{Bmatrix} u \\ v \end{Bmatrix} = \mathbf{N}_m \mathbf{q}_m^e, \quad (6)$$

where \mathbf{N}_m = the appropriate interpolation functions matrix, while the non-conforming bending deformations are²

$$w^* = \mathbf{N}_b \mathbf{q}_b^e + \left\langle \frac{1}{2} x^2 \quad \frac{1}{2} y^2 \quad \frac{1}{2} xy \right\rangle (\mathbf{B}_c - \mathbf{B}_0) \mathbf{q}_b^e = \mathbf{N}_b^* \mathbf{q}_b^e, \quad (7)$$

which leads to the refined strain matrix for the non-conforming bending element as $\mathbf{B}_b^* = \mathbf{B}_b + \mathbf{B}_c - \mathbf{B}_0$, for which

$$\mathbf{B}_c = \mathbf{B}'_c + \lambda (\mathbf{B}'_c - \mathbf{B}_c^*), \quad (8)$$

where the RT9 formulation adopts a value of $\lambda = 0.25$ for the adjustable parameter λ .

The global statement of (5) becomes

$$(\mathbf{K} + \mathbf{K}_\sigma) \Delta \mathbf{q} = {}^{t+\Delta t} \mathbf{P} - {}^t \mathbf{R}, \quad (9)$$

with ${}^{t+\Delta t} \mathbf{P}$ and ${}^t \mathbf{R}$ being the external equivalent nodal load vector at time $t + \Delta t$ and the internal load vector at time t respectively.

An incremental-iterative full Newton-Raphson method, in which the tangent stiffness matrix is updated in each iteration for each load increment, is employed to produce a rapidly convergent solution. The effect of cracking is treated by changing the material properties of the cracked element. In the solution procedure, as the stresses may redistributed during an iteration, some cracks may close, which may lead to numerical instability. To overcome this problem, closure and re-opening of the cracks are allowed in the present analysis and the material property matrix is updated according to the appropriate material states. The loading is divided into a series of load increments, and in the present investigation, load increments are generated automatically to model the nonlinear behaviour more efficiently. Among the various approaches suggested to obtain changing load increments, the increment load factor is set to

$$\Delta \lambda_n = \Delta \lambda_{n-1} \sqrt{\frac{N_d}{N_{n-1}}}, \quad (10)$$

where $\Delta \lambda_{n-1}$ = load increment factor of the last increment, N_{n-1} = number of iterations in the last load increment step, N_d = desired number of iterations ($N_d \approx 3-5$), and $\Delta \lambda_n$ = load increment factor of the current increment. Using this approach, the load increment can be prescribed as being larger at the initial linear stage and smaller when the response starts to become more nonlinear.

6 NUMERICAL EXAMPLES

Two numerical examples are chosen to validate the solution and to demonstrate the

efficiency of the element, these being the slabs tested by McNeice⁵ and Duddeck⁶. Figure 1 shows the results of the present method compared with the tests of Ref. 6, as well as the numerical solutions of other investigators. Additionally, accurate solutions were predicted for the slab of Ref. 5.

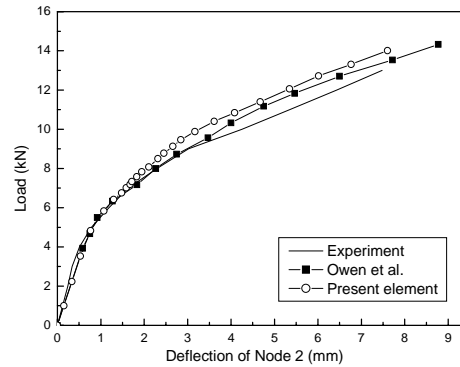


Figure 1: Slab tested by Duddeck⁶

12 CONCLUSIONS

- The paper presents a combining of efficient 9-dof 3-node membrane and 9-dof 3-node non-conforming plate bending elements to produce an 18-dof triangular element for the nonlinear analysis of RC slabs.
- The formulation uses a layered approach, and includes concrete cracking and biaxial stress states. Tension stiffening and aggregate interlock effects are included.
- The solutions compare favourably with tests, and the element performance is good.

REFERENCES

- [1] D.J. Allman, "A compatible triangular element including vertex rotations for plane elasticity analysis", *Comps. & Structs.*, **19**, 1-8 (1984).
- [2] Y.K. Cheung and W.J. Chen, "Refined nine-parameter triangular thin plate bending element by using refined direct stiffness method", *Int. J. Num. Meth. Engng*, **38**, 283-298 (1995).
- [3] L. Cedolin and S. Deipoli, "Finite element studies of shear-critical R/C beams", *J. Eng. Mechs, ASCE*, **103**(EM3), 395-410 (1977).
- [4] J. Izumo, H. Shin, K. Meakawa and H. Okamura, "An analytical model for PC panels subjected to in-plane stresses, *Concrete shear in earthquakes*, Elsevier, London (1992).
- [5] G.M. McNeice *Elastic-plastic bending of plates and slabs by the finite element method*, Ph.D thesis, University of London (1967).
- [6] H. Duddeck, G. Griebenou and G. Schaper, "Material and time dependent non-linear behavior of cracked reinforced concrete slabs-Finite element analysis and laboratory tests", *Non-linear behavior of reinforced concrete spatial structures-Prelim Report 1*, Düsseldorf, 101-113 (1978).

